High Temperature. Vol. 44, No. 3, 2006, pp. 364–372. Translated from Teplofizika Vysokikh Temperatur, Vol. 44, No. 3, 2006, pp. 370–377.

THERMOPHYSICAL PROPERTIES OF MATERIALS

Molecular-Dynamic Calculation of Spectral Characteristics of Absorption of Infrared Radiation by $(H_2O)_j$ and $(CH_4)_i(H_2O)_n$ Clusters

A. E. Galashev, V. N. Chukanov, A. N. Novruzov, and O. A. Novruzova

Institute of Environmental Engineering, Ural Division of the Russian Academy of Sciences, Ekaterinburg, Russia

Received January 11, 2005

Abstract—The method of molecular dynamics is used to investigate the stability and physical properties of $(CH_4)_i(H_2O)_n$ clusters. The possibility of methane molecules being absorbed by clusters containing ten and twenty water molecules is demonstrated. Such clusters retain the thermodynamic stability when the number of CH_4 molecules they absorbed does not exceed six. The frequency dispersion of complex permittivity of $(CH_4)_i(H_2O)_n$ aggregates reflects the resonant behavior of polarizability depending on the applied electric field. The dependence of the absorption coefficient α on the frequency of infrared radiation varies significantly after even one CH_4 molecule is absorbed by water clusters. The maximal value of α for water aggregates which absorbed CH_4 molecules is much lower than the respective value for pure water clusters of appropriate size.

INTRODUCTION

Important information about the structure, dynamics, and chemical bonds of molecules may be obtained on the basis of the data on infrared spectroscopy which was used in [1] to study molecular complexes with combined use of lasers and molecular beam technology. Direct measurements of the absorption coefficient involve transmitting a laser ray through a molecular beam and recording the absorption of laser radiation at different frequencies. A signal which corresponds to the decrease in the laser beam intensity is given by the expression [2]

$$\delta I = I_0 \exp(-\alpha L), \qquad (1)$$

where I_0 is the intensity of laser radiation, α is the absorption coefficient, and L is the path length over which the radiation interacts with the substance being investigated. The sensitivity of this method is limited by the detector noise and amplitude fluctuations developed by the laser.

Characteristic frequencies of oscillation in the absorption spectrum $\alpha(\omega)$ correspond to certain bonds, to groups of bonds in a molecule, and to a certain spatial structure of a molecule. Such frequencies enable one to draw inferences about the structure of molecules [3]. A simple example of the impact made by rotation of a molecule on its spectrum is provided by methane molecule which has tetrahedral equilibrium geometry in the ground state and is characterized by the absence of dipole moment. The distortion, which arises during rotation of this molecule, leads to the emergence of nonzero dipole moment, and the CH_4 molecule acquires a rotational spectrum. Because of the small mass of hydrogen atoms, the frequencies of stretching vibrations of the C–H bond are in the range of 3000–3500 cm^{-1} [3]. The frequencies of variation of H–C–H angles are about 1400 cm^{-1}, the average valence frequency of water molecule is 3700 cm^{-1}, and the deformation frequency is 1600 cm^{-1}. In the Earth atmosphere, the "spherical top" of CH_4 is recorded most clearly in the vicinity of the frequency of 3062 cm^{-1} [4]. The water molecule is an asymmetric top with a very rich absorption spectrum from the far infrared to visible. Note that the rotation is not necessarily accompanied by the emergence of an infrared absorption band. The absorption occurs only when the rotation leads to a variation of

0018-151X/06/4403-0364

the charge distribution within the molecule. In condensed systems (with which clusters may be classed), spectra are induced owing to intermolecular interactions, which are associated with dipole transitions forbidden by the selection rules for isolated molecules [5]. In the long-wave IR regions, translational spectra are located which represent a special type of induced spectra. The translational absorption is associated with a dipole moment arising as a result of deformation of electron shells in collisions. For the majority of nonpolar molecules, the induced translational and rotational spectra are located in one and the same frequency range and cannot be observed separately [5]. In the case of bulk water, it is assumed that motions with a frequency less than 1200 cm^{-1} correspond to molecular vibrations, and frequencies above 1200 cm^{-1} describe largely intramolecular vibrations [6]. As a rule, the induction interaction is treated within the dipole interaction. This interaction is attractive. The induction energy is always negative and anisotropic, because it depends on the direction of dipole moment and on the direction of applied field.

In a linear approximation, the electric induction vector D is determined in terms of the electric field vector E using the coefficient ε (permittivity). The treatment of the time dependence of the system reaction [7] defines the need to introduce the complex permittivity.

The method of molecular dynamics enables one to calculate the IR spectra of systems formed by polar molecules. The IR spectra are used to determine the system dynamics. If it turns out that the dynamics of molecules in clusters and in massive substance are by and large identical, systems containing only several molecules may be used for detailed investigation of the dynamic properties of this substance. Water is of great interest for the purposes of investigation, because it exhibits unique physical properties and is a model liquid with hydrogen bonds. In spite of the fact that the physical properties of water are intensively investigated using the methods of computer modeling, the microscopic dynamics of H_2O have been investigated inadequately. Only isolated studies are known dealing with molecular-dynamic calculation of IR spectra of water clusters [8] and water aggregates containing molecules of greenhouse gases (CO_2, N_2O) [9].

Both water vapor and methane are among the most significant greenhouse gases which retain heat in the Earth atmosphere. The main contribution to the greenhouse effect is made by atmospheric water vapor. The methane fraction among other gases in the greenhouse effect (disregarding H_2O vapors) is estimated at 7.2% [10]. The bulk of atmospheric water vapor is located in the lower part of the atmosphere (troposphere) [11]. The capacity of water droplets moving in the troposphere to absorb impurity is known [12]. The optical effect associated with the clusterization of water vapor has not been investigated.

Parameters of the potential and geometry of H_2O and CH_4 molecules

H_2O		CH_4	
Parameters	Values	Parameters	Values
σ, nm	0.3234	σ, nm	0.3817
ε, eV	0.007935	ε, eV	0.0128067
r_{OH}, nm	0.09572	r_{CH}, nm	0.1091
Δ_{HOH}, deg.	104.52	Δ_{HCH}, deg.	109.3
q_O, e	0	q_H, e	0.116
q_H, e	0.5190	q_C, e	–0.464
q_M, e	–1.0380		
d, D	1.848	d, D	0
α, Å^3	1.4440	α, Å^3	2.6

It is our objective to study the thermodynamic stability and time dispersion of complex permittivity of $(H_2O)_n$ and $(CH_4)_i(H_2O)_n$ clusters, as well as to investigate the absorption spectra of these aggregates under conditions which are characteristic of the troposphere.

COMPUTER MODEL

Water clusters are modeled using the TIP4P refined interaction potential for water and a rigid four-center model of H_2O molecule [13]. The geometry of this molecule corresponds to the experimental data on the bond distances of molecule in the gas phase [14]. Fixed charges (see table) are ascribed to H atoms and to point M lying on the bisectrix of angle HOH at a distance of 0.0215 nm from the oxygen atom. The values of charges and the position of point M are selected so as to reproduce the experimentally obtained values of dipole and quadrupole moments [15, 16], as well as the dimer energy obtained in calculations *ab initio* and characteristic distances in the dimer [17]. The parameters of the Lennard–Jones potential introduced for taking short-range interactions into account are ascribed to the oxygen atom. Related to point M in

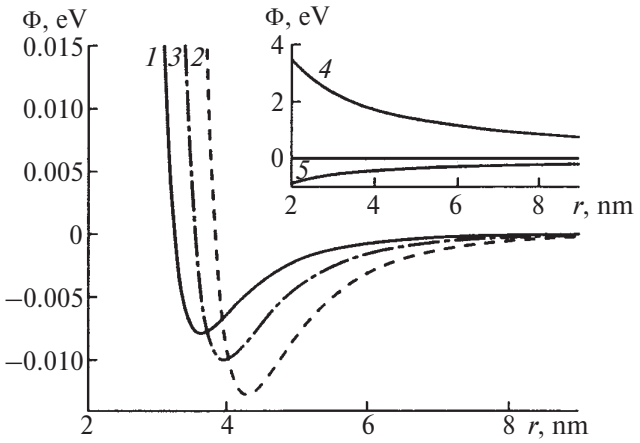

Fig. 1. (*1–3*) The Lennard–Jones and (*4*, *5*) the Coulomb potentials, which represent the additive part of interactions: (*1*) H_2O–H_2O, (*2*) CH_4–CH_4, (*3*) H_2O–CH_4, (*4*) C–O, (*5*) C–H in $(CH_4)_i(H_2O)_n$ clusters.

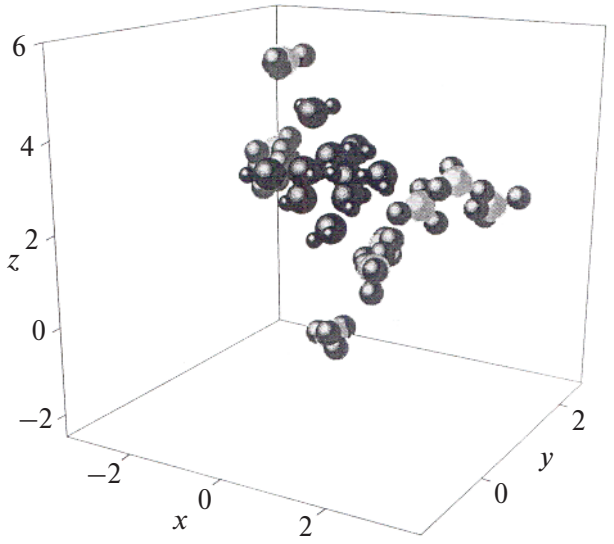

Fig. 2. The configuration of $(CH_4)_3(H_2O)_{10}$ cluster, which corresponds to the time instant of 20 ps.

addition to the electric charge is the polarizability which is required for the description of nonadditive polarization energy.

The total energy of interaction between water molecules is written as

$$U_{\text{tot}}^{(1)} = U_{\text{pair}} + U_{\text{pol}}, \qquad (2)$$

where the pair-additive part of the potential is the sum of Lennard-Jones and Coulomb interactions,

$$U_{\text{pair}} = \sum_i \sum_j \left(4\varepsilon \left[\left(\frac{\sigma_{ij}}{r_{ij}} \right)^{12} - \left(\frac{\sigma_{ij}}{r_{ij}} \right)^{6} \right] \right) + \frac{q_i q_j}{r_{ij}}. \qquad (3)$$

Here r_{ij} is the distance between points i and j, q is the charge, and σ and ε are parameters of the Lennard–Jones potential.

The nonadditive polarization energy is defined by the relation

$$U_{\text{pol}} = -\frac{1}{2} \sum_i \mathbf{d}_i \mathbf{E}_i^0, \qquad (4)$$

where $\mathbf{E}_i^0$ is the electric field intensity at point i produced by fixed charges located in the system,

$$\mathbf{E}_i^0 = \sum_{j \neq i} \frac{q_j \mathbf{r}_{ij}}{r_{ij}^3}, \qquad (5)$$

and $\mathbf{d}_i$ is the induced dipole moment of atom i,

$$\mathbf{d}_i = \alpha_i \mathbf{E}_i, \qquad (6)$$

where

$$\mathbf{E}_i = \mathbf{E}_i^0 + \sum_{j \neq i} \mathbf{T}_{ij} \cdot \mathbf{d}_j. \qquad (7)$$

Here, $\mathbf{E}_i$ is the intensity of total electric field at the center of atom i, α is the atomic polarizability, and $\mathbf{T}_{ij}$ is the dipole tensor,

$$\mathbf{T}_{ij} = \frac{1}{r_{ij}^3} \left(\frac{3 \mathbf{r}_{ij} \mathbf{r}_{ij}}{r_{ij}^2} - 1 \right). \qquad (8)$$

The standard iterative procedure is used at every time step to calculate induced dipole moments [13]. The accuracy of determination of $\mathbf{d}_i$ is preassigned in the range of 10^{-5}–10^{-4} D.

The interaction between CH_4 and H_2O molecules was calculated by an identical scheme, i.e., using formulas (2)–(8). The potential functions used in this case are represented in detail in [18]. The parameters of the potential functions are given in the table. Individual components of the additive part of the potential, which describes the interaction of molecules in the model, are given in Fig. 1. The Lennard–Jones potential for the improved TIP4P model [13] of water (curve *1*) has a somewhat deeper potential well than the potential of the previous model [19]. The location of the potential minimum is defined by the distance $r_{\min} = 2^{1/6}\sigma_1 = 0.363$ nm. The LD component of the potential characterizing the interaction between CH_4 molecules (curve *2*) has a still deeper potential well,

and the location of the minimum is given by r_{min} = = 0.428 nm. The parameters of the LD component of the potential function describing the interactions of CH_4 molecules with H_2O are determined as σ_3 = = $(\sigma_1 + \sigma_2)/2$ and $\varepsilon_3 = \sqrt{\varepsilon_1 \varepsilon_2}$. The profile of this function takes the intermediate position between curves *1* and *2*. The potentials of Coulomb interaction between a carbon atom and atoms of water molecules are shown in the inset of Fig. 1 (curves *4* (C–O) and *5* (C–H)). The carbon atom in the CH_4 molecule has a negative electric charge.

Figure 2 gives the configuration of $(CH_4)_9(H_2O)_{10}$ cluster, which relates to the time instant of 20 ps. The stratification of molecules of different sorts is observed in this aggregate, namely, ten H_2O molecules along with three CH_4 molecules take up one part of space, and six CH_4 molecules take up the other part. It will be shown below that such a structure is thermodynamically unstable.

A CH_4 molecule is shaped as a tetrahedron with a carbon atom at the center and hydrogen atoms at the vertexes. This molecule has rotoflection tetrad axes [20]. The parameters which preassign the geometry of CH_4 molecule [21] and its physical properties [18] are given in the table.

The Gear method of the fourth order [22] was used to determine the trajectories of the centers of mass of molecules. The integration time step Δt was 10^{-17} s. First, in a molecular-dynamic calculation with a duration of 2×10^6 Δt, the equilibrium state at $T = 233$ was prepared for water clusters which contained no impurity molecules. The water cluster configuration relating to the instant of time of 20 ps was subsequently used as the initial configuration for modeling the $(CH_4)_i(H_2O)_n$ system. The CH_4 molecules being added were first arranged such that the least distance between atoms in methane molecule and atoms of water molecules would be at least 0.6 nm. The CH_4 molecules were initially arranged in two ways. When the number of CH_4 molecules being added did not exceed six, the impurity molecule was arranged such that its triad would coincide with the ray connecting the center of mass of $(H_2O)_n$ cluster to the center of mass of this molecule. In so doing, the hydrogen atoms which belonged to the base of tetrahedral molecule (triangular pyramid) were closer to the center of mass of $(H_2O)_n$ cluster than the hydrogen atoms at the vertex of the pyramid. The rays were provided by the axes of Cartesian coordinates whose center 0 was coincident with the cluster center of mass. In the case of more than six CH_4 molecules, the center of the seventh and subsequent molecules coincided with a bcc-lattice site spaced at a distance of at least 0.5 nm from atoms of the molecules closest to this site (H_2O and CH_4). One such lattice site was coincident with the center of mass of $(H_2O)_n$ cluster. The orientation of the molecules located at bcc-lattice sites was arbitrary. The cut-off radius of all interactions in the model was 0.9 nm. The newly formed system was balanced during the time interval $0.6\times10^6\Delta t$, and then the necessary physicochemical properties were calculated during the interval $2\times10^6\Delta t$. The Rodriguez–Hamilton parameters [23] were used to derive the analytical solution of equations of motion for molecular rotation, and the scheme of integration of the equation of motion in the presence of rotations corresponded to the approach suggested by Sonnenschein [24].

The results of molecular-dynamic calculations involving the use of various empirical potentials do not yet enable one to draw a conclusion as to which structure of $(H_2O)_{20}$ cluster corresponds to the minimal energy. Fanourgakis *et al.* [25] performed high-level *ab initio* calculations to demonstrate that the structure of $(H_2O)_{20}$ cluster, which is most advantageous energetically, is formed on the basis of a pentagonal prism (U_{tot} = –(899.4–911.5) kJ/mol) rather than a dodecahedron (–837.0 kJ/mol) or fused cubes (–889.3 kJ/mol). The internal energy of structure of $(H_2O)_{20}$ cluster in the model presented by us is –836.0 kJ/mol.

The calculations were performed in a Pentium-IV computer with a clock frequency of the processor of 1.8 GHz. A calculation with a duration of $10^6\Delta t$ for cluster of 30 molecules required about 70 hours of computer time.

SPECTRAL CHARACTERISTICS OF $(H_2O)_n$ AND $(CH_4)_i(H_2O)_n$ CLUSTERS

The total dipole moment of cluster is preassigned in the form

$$\mathbf{M}(t) = \sum_{i=1}^{N} \mathbf{d}_i(t),$$

where $d_i(t)$ is the dipole moment of molecule i, and N is the number of molecules in the cluster.

The static permittivity ε_0 was calculated in terms of fluctuations of the total dipole moment [26],

$$\varepsilon_0 = 1 + \frac{4\rho}{3VkT}[\langle \mathbf{M}^2 \rangle - \langle \mathbf{M} \rangle^2].$$

We introduce the Fourier–Laplace transform of the function f in terms of the relation

$$L_{i\omega}[f] = \int_0^\infty (dt \exp(-i\omega t)) f(t)$$

and normalized autocorrelation function M using the equality

$$\Phi(t) = \langle \mathbf{M}(0) \cdot \mathbf{M}(t) \rangle / \langle \mathbf{M}^2 \rangle .$$

The frequency dependence of permittivity is represented in the form of complex quantity $\varepsilon(\omega) = \varepsilon'(\omega) - \varepsilon''(\omega)$ with the real part $\varepsilon'(\omega)$ (dielectric dispersion) and imaginary part $\varepsilon''(\omega)$ which characterizes dielectric loss. The correlation between the frequency-dependent permittivity and the Fourier–Laplace transform for the time derivative of the function Φ is defined by the relation [26]

$$L_{i\omega}[-\Phi] = \frac{\varepsilon(\omega) - 1}{\varepsilon_0 - 1} = 1 - i\omega L_{i\omega}[\Phi].$$

The quantity ε_0 is found in terms of the function $\varepsilon(\omega)$: $\varepsilon_0 = \varepsilon(0)$.

A molecule may absorb electromagnetic waves of certain frequency only in the case where the dipole moment of the molecule performs vibrations with the same frequency. The absorption coefficient is proportional to the square of the amplitude of vibration of the dipole moment. The absorption of radiation on frequency ω at thermodynamic equilibrium in the gas phase with temperature T is characterized by the absorption coefficient α. The quantity α may be represented in terms of the imaginary part of the frequency-dependent permittivity $\varepsilon(\omega)$ in the form [27]

$$\alpha(\omega) = 2\frac{\omega}{c}\mathrm{Im}[\varepsilon(\omega)^{1/2}],$$

where c is the velocity of light.

CALCULATION RESULTS

The thermodynamic stability of water clusters which absorbed CH_4 molecules was investigated using the criterion [28]

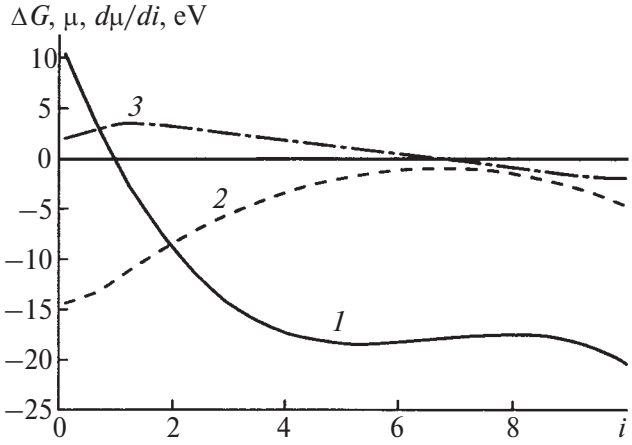

Fig. 3. (*1*) The excess free energy ΔG, (*2*) the chemical potential μ, and (*3*) the stability coefficient $(\partial\mu/\partial i)_{P,T}$ as functions of the number of CH_4 molecules in $(CH_4)_i(H_2O)_{10}$ clusters.

$$(\partial\mu/\partial i)_{P,T} > 0. \quad (9)$$

The dependence of excess free energy ΔG, chemical potential μ, and stability coefficient $(\partial\mu/\partial i)_{P,T}$ on the number i for $(CH_4)_i(H_2O)_{10}$ clusters is given in Fig. 3. The value of ΔG (curve *1*) decreases rapidly with i varying from zero to four, and passes a shallow minimum in the neighborhood of $i = 5$ and a sloping maximum at $i = 8$. The chemical potential μ increases with i and decreases again starting with $i = 7$. At $i \geq 6$, $(\partial\mu/\partial i)_{P,T} < 0$, i.e., criterion (9) predicts that $(H_2O)_{10}$ cluster is stable relative to the absorption of CH_4 molecules up to the increase in its size by six CH_4 molecules. As to large-size clusters, $(CH_4)_i(H_2O)_{20}$ aggregates which add more than six CH_4 molecules turn out to be thermodynamically unstable.

The variation of energy E_{a-a} of interaction between CH_4 molecules in $(CH_4)_i(H_2O)_{10}$ and $(CH_4)_i(H_2O)_{20}$ clusters is given in Fig. 4. Up to $i = 4$, the CH_4–CH_4 interaction in clusters of both types is very weak. This is associated with the initial symmetric arrangement of CH_4 molecules around water clusters, when all CH_4 molecules were wide apart. While the distance between C and O atoms in the initial configurations of aggregates containing up to six CH_4 molecules was 0.613 nm, the distance between C and C atoms was 1.477 nm, i.e., exceeded the cut-off radius of all interactions. So long as the number of CH_4 molecules was less than four ($i \leq 4$), the distances between them did not exceed the location of minimum

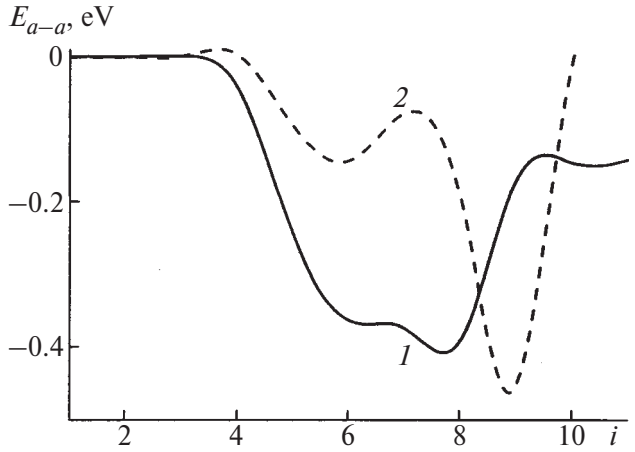

Fig. 4. The energy of CH_4–CH_4 interaction as a function of the number of methane molecules in (*1*) $(CH_4)_i(H_2O)_{10}$ and (*2*) $(CH_4)_i(H_2O)_{20}$ clusters.

for the potential describing their interaction. The addition of a fifth CH_4 molecule to the clusters is accompanied by a significant decrease in energy E_{a-a}. In clusters of both types, the initial decrease in energy E_{a-a} occurs until six CH_4 molecules are added to the clusters. Further pattern of the dependence $E_{a-a}(i)$ differs for $(CH_4)_i(H_2O)_{10}$ and $(CH_4)_i(H_2O)_{20}$ clusters. For clusters of the former type, the dependence $E_{a-a}(i)$ (curve *1*) passes a sloping maximum ($i = 7$) and a minimum ($i = 8$), and increases rapidly when a ninth CH_4 molecule is added to the cluster. This high value is retained up to $i = 11$. For clusters of the latter type, the dependence $E_{a-a}(i)$ (curve *2*) reaches a local maximum at $i = 7$ and deep minimum at $i = 9$.

The frequency dependences of the real and imaginary parts of permittivity for $(CH_4)_i(H_2O)_{20}$ clusters with $i = 1, 4$, and 8 are given in Fig. 5. One can see that the values of both the real and imaginary parts of $\varepsilon(\omega)$ decrease as CH_4 molecules are added to a water cluster. The form of dependences $\varepsilon'(\omega)$ and $\varepsilon''(\omega)$ corresponds to the process of transition to polarization in time. The dying oscillation of the polarization vector **P** is defined as resonant and corresponds to the behavior of the functions $\varepsilon'(\omega)$ and $\varepsilon''(\omega)$ shown in Fig. 5. Figure 5b makes it possible to obtain information about frequencies which are active in IR absorption. The frequency characteristic of IR absorption varies insignificantly with the size of $(CH_4)_i(H_2O)_{20}$ clusters because of absorption of CH_4 molecules and is 270 cm^{-1} at $i = 1$ and 260 cm^{-1} at $i = 4$ and 8.

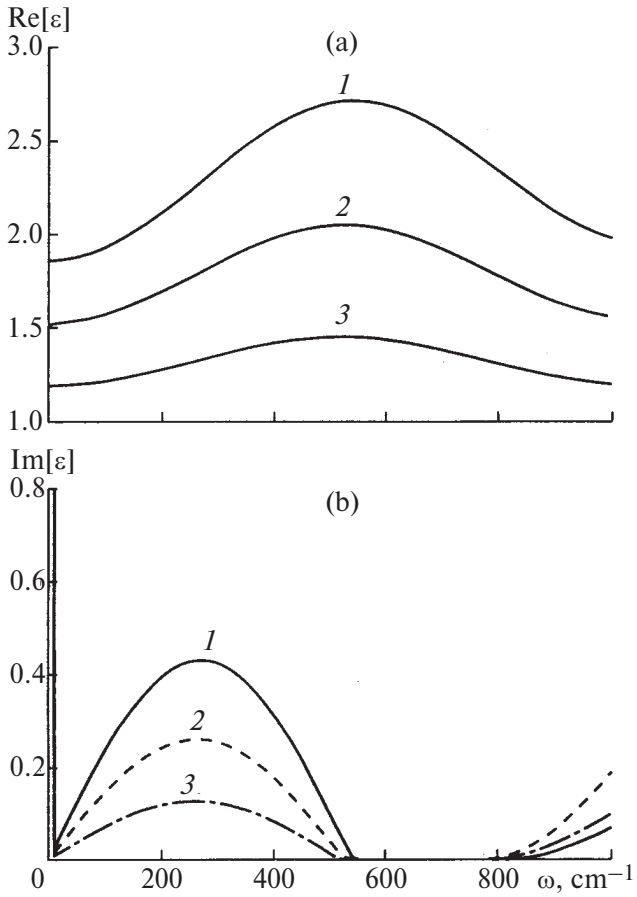

Fig. 5. The frequency dependence of the (a) real and (b) imaginary parts of permittivity of $(CH_4)_i(H_2O)_{20}$ clusters: (*1*) $i = 1$, (*2*) 4, (*3*) 8.

The frequency dependence of the absorption coefficient $\alpha(\omega)$ of $(CH_4)_i(H_2O)_{20}$ clusters with $i = 1, 5$, and 9 is compared to the function $\alpha(\omega)$ for $(H_2O)_{20}$ cluster and to the respective experimentally obtained dependence for bulk water [29] in Fig. 6. One can see in Fig. 6 that the form of the function $\alpha(\omega)$ varies significantly after even one CH_4 molecule is absorbed by water cluster. Further increase in the number of molecules being absorbed leads to a more intensive decrease in $\alpha(\omega)$ in the frequency range under consideration ($0 \le \omega \le 1000$ cm^{-1}). The IR radiation in the frequency range $540 \le \omega \le 800$ cm^{-1} is not at all absorbed by clusters which absorbed at least one CH_4 molecule. The reaction of $(H_2O)_{20}$ cluster to an electric field which is uniform in space and variable in time is most effective on frequencies $\omega_1 = 721$ cm^{-1} and $\omega_2 = 1037$ cm^{-1}. The $\alpha(\omega)$ spectrum for bulk water exhibits a higher intensity than the similar dis-

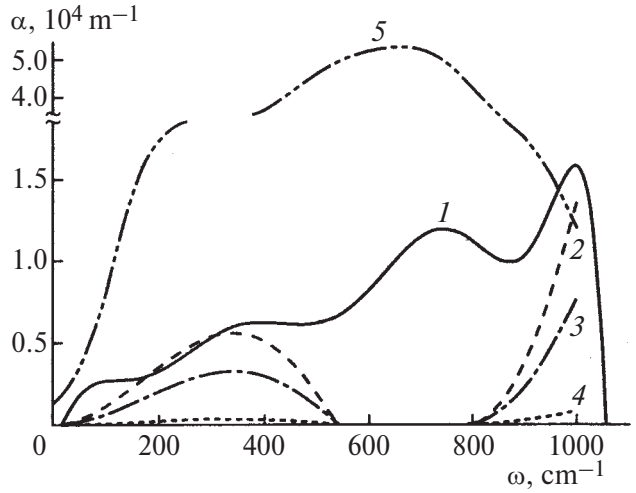

Fig. 6. The absorption coefficient α determined in terms of frequency-dependent permittivity for $(CH_4)_i(H_2O)_{20}$ clusters at: (*1*) i = 0, (*2*) 1, (*3*) 5, (*4*) 9, (*5*) experimentally obtained α(ω) spectrum for bulk water [29].

tribution for clusters. In the case of bulk water, the main frequencies of absorption of IR radiation may also be identified: $\omega_1 = 200$ cm^{-1} and $\omega_2 = 700$ cm^{-1}. $(CH_4)_i(H_2O)_{20}$ clusters exhibit one characteristic frequency of absorption of IR radiation. When the number of molecules CH_4 in a cluster is $i = 1$, this frequency is 370 cm^{-1}, and for $i = 5$ and 9 it is 340 cm^{-1}. The increase in the absorption coefficient of $(CH_4)_i(H_2O)_{20}$ clusters with frequency at $\omega \geq \geq 800$ cm^{-1} (see Fig. 6) infers that the α(ω) spectrum of these aggregates continues to the frequency range with $\omega > 1000$ cm^{-1}. However, for correctly determining the dependence α(ω) in this range of values of (ω), it is necessary to explicitly include the intramolecular vibrations.

The frequency ω_α, which corresponds to the maximal values of the coefficient α for $(H_2O)_i$, $(CH_4)_i(H_2O)_{10}$, and $(CH_4)_i(H_2O)_{20}$ clusters, is given in Fig. 7a. One can see that small clusters of pure water with the number of molecules $2 \leq i \leq 11$ have the fundamental frequencies of absorption of IR radiation in the range $690 \leq \omega_\alpha \leq 990$ cm^{-1}. The clusters, whose size increased owing to the absorption of CH_4 molecules, are characterized by significantly lower fundamental frequencies of absorption, namely, $320 \leq \omega_\alpha \leq \leq 380$ cm^{-1}. In so doing, a smoother $\omega_\alpha(i)$ dependence

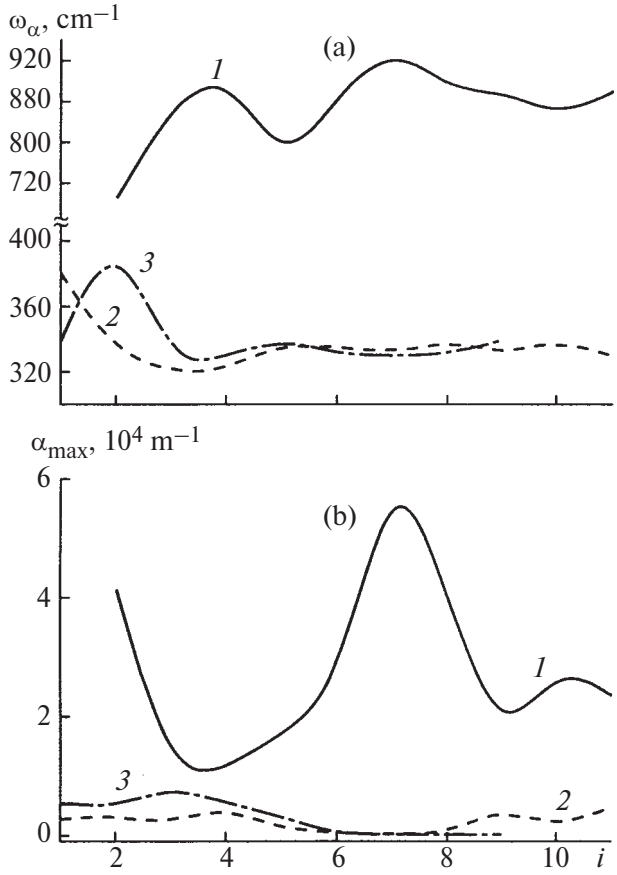

Fig. 7. (a) The frequency corresponding to the maximal value of the absorption coefficient and (b) the maximal values of the absorption coefficient α of the clusters as functions of the number of molecules i (H_2O or CH_4) in (*1*) $(H_2O)_i$, (*2*) $(CH_4)_i(H_2O)_{10}$, and $(CH_4)_i(H_2O)_{20}$ clusters.

is observed for clusters with ten water molecules. In this case, ω_α decreases rapidly with the number i varying from unity to three and, at $i > 3$, fluctuates weakly in the vicinity of 335 cm^{-1}. For $(CH_4)_i(H_2O)_{20}$ clusters, ω_α passes a maximum at $i = 2$ and then, at $i > 3$, fluctuates from the average value (335 cm^{-1}) with a deviation of 5 cm^{-1}. A variation with the number i of the absorption coefficient α_{max} corresponding to the principal maximum of the function α(ω) for $(H_2O)_i$, $(CH_4)_i(H_2O)_{10}$, and $(CH_4)_i(H_2O)_{20}$ clusters is given in Fig. 7b. One can see that the values of α_{max} for the smallest ($2 \leq i \leq 11$) clusters of water are higher than the respective characteristics for all clusters considered here, including the largest aggregates $(CH_4)_i(H_2O)_{20}$. Up to the addition of six CH_4 molecules (i = 6), the values of α_{max} for

$(CH_4)_i(H_2O)_{20}$ clusters are higher than those for $(CH_4)_i(H_2O)_{10}$ aggregates. However, at $i \geq 8$, the value of α_{max} for small clusters becomes higher than that for large clusters.

CONCLUSIONS

We have demonstrated that water clusters containing 10 and 20 molecules may absorb up to six molecules of methane while remaining stable. The pattern of interaction between CH_4 molecules depends both on the number of absorbed molecules of methane and on the number of water molecules in clusters. The calculated frequency dispersion of permittivity exhibits a resonant pattern. Hence follows that the interaction between electromagnetic wave and dipole moment of $(CH_4)_i(H_2O)_n$ clusters likewise proceeds by the resonant mechanism. A significant feature of resonance exchange in wave processes is that the mean probability of exchange increases with temperature [30]. Indeed, the pattern of resonant interaction largely depends on the ratio between the period of exchange $1/\Omega$ and time of interaction τ. The transfer of the electromagnetic wave energy is realized under conditions of $\Omega\tau << 1$. The temperature dependence of probability of transition is defined by the behavior of $(\Omega\tau)^2$ as a function of temperature. The time of interaction is preassigned by the size of cluster. In the process under consideration, this time may be taken to be independent of temperature, while $\Omega \sim kT$.

The dissolution of nonpolar or weakly polar substances in water leads to the effect of "mutual relaxation" [31]. The interaction between CH_4 molecules is largely caused by dispersion Van der Waals forces and is weaker than the interaction in the case of highly polar dipole substances such as water. The "relaxation" effect is found in water clusters containing CH_4 molecules.

After water clusters absorb at least one methane molecule, the frequency dependence of absorption coefficient varies significantly. The number of maxima in the $\alpha(\omega)$ dependence is reduced from two to one; this is accompanied by a decrease in the frequency that is most active in the absorption of IR radiation. An analogy is observed with the infrared absorption spectrum of xenon hydrate [32] obtained using high-resolution experimental equipment. The far infrared region of this spectrum contains a wide absorption band in the range between 100 and 330 cm^{-1} with a maximum at 235 cm^{-1}. The translational motion of water molecules predominates in this region. Tse and Klein [32] note that the frequencies which characterize the motion of xenon atoms are lower than the frequencies which correspond to translational motions of methane in a similar structure I of methane hydrate. After the absorption of methane molecules by water clusters, the intensity of IR radiation absorbed by them with a frequency $\omega \leq 800$ cm^{-1} decrease significantly.

In time, a cluster may grow to a microdroplet. In this case, the highly curved surface on the droplet-air interface acts as a lens, i.e., it focuses the radiation incident on some small region within the droplet. In other words, a temperature field with a high gradient arises in the inner region of the droplet, the so-called hot spot. In this case, the probability of emergence of nonlinear optical processes increases.

ACKNOWLEDGMENTS

This study was supported by the Russian Foundation for Basic Research (Yugra grant nos. 03-02-96807 and 04-02-17322).

REFERENCES

1. Pine, A.S. and Lafferty, W.J., *J. Chem. Phys.*, 1983, vol. 78, p. 2154.
2. Havenith, M., *Infrared Spectroscopy of Molecular Clusters*, Berlin: Springer, 2002.
3. El'yashevich, M.A., *Atomnaya i molekulyarnaya spektroskopiya* (Atomic and Molecular Spectroscopy), Moscow: Gos. Izd. Fiz.-Mat. Lit., 1962.
4. Antipov, A.B., Kapitanov, V.A., Ponomarev, Yu.N., and Sapozhnikova, V.A., *Optiko-akusticheskii metod v lazernoi spektroskopii atmosfernykh gazov* (Optico-Acoustic Method in Laser Spectroscopy of Atmospheric Gases), Novosibirsk: Nauka, 1984.
5. *Spektroskopiya vzaimodeistvuyushchikh molecul* (The Spectroscopy of Interacting Molecules), Bulanin, M.O., Ed., Leningrad: Izd. LGU (Leningrad State Univ.), 1970.
6. Stern, H.A. and Berne, B.J., *J. Chem. Phys.*, 2001, vol. 115, p. 7622.
7. Bredov, M.M., Rumyantsev, V.V., and Toptygin, I.N., *Klassicheskaya elektrodinamika* (Classical Electrodynamics), St. Petersburg: Lan', 2003.
8. Bosma, W.B., Fried, L.E., and Mukamel, S., *J. Chem. Phys.*, 1993, vol. 98, p. 4413.
9. Chukanov, V.N. and Galashev, A.E., *Perspekt. Energ.*, 2003, vol. 7, p. 283.
10. Halmann, M.M. and Steinberg, M., *Greenhouse Gas Carbon Dioxide Mitigation. Science and Technology*, Boca Raton: Lewis Publ., 1999.

11. Peng, G., Leslie, L.M., and Shao, Y., *Environmental Modeling and Prediction*, Berlin: Springer, 2002.
12. Galashev, A.E., Pozharskaya, G.I., and Chukanov, V.N., *Kolloidn. Zh.*, 2002, vol. 64, no. 6, p. 762.
13. Dang, L.X. and Chang, T.-M., *J. Chem. Phys.*, 1997, vol. 106, p. 8149.
14. Benedict, W.S., Gailar, N., and Plyler, E.K., *J. Chem. Phys.*, 1956, vol. 24, p. 1139.
15. Xantheas, S., *J. Chem. Phys.*, 1996, vol. 104, p. 8821.
16. Feller, D., and Dixon, D.A., *J. Chem. Phys.*, 1996, vol. 100, p. 2993.
17. Smith, D.E. and Dang, L.X., *J. Chem. Phys.*, 1994, vol. 100, p. 3757.
18. Sun, Y., Spellmeyer, D., Pearlman, D.A., and Kollman, P., *J. Am. Chem. Soc.*, 1992, vol. 114, p. 6798.
19. Caldwell, J., Dang, L.X., and Kollman, P.A., *J. Am. Chem. Soc.*, 1990, vol. 112, p. 9144.
20. Mayants, L.S., *Teoriya i raschet kolebanii molekul* (The Theory and Calculation of Molecular Vibrations), Moscow: Izd. AN SSSR (USSR Acad. Sci.), 1960.
21. *Spravochnik khimika* (Chemist's Handbook), Nikol'skii, B.P., Ed., Leningrad: Khimiya, 1971, vol. 1.
22. Haile, J.M., *Molecular Dynamics Simulation. Elementary Methods*, New York: Wiley, 1992.
23. Koshlyakov, V.N., *Zadachi dinamiki tverdogo tela i prikladnoi teorii giroskopov* (Problems in Dynamics of Solid and Applied Theory of Gyroscopes), Moscow: Nauka, 1985.
24. Sonnenschein, R., *J. Comp. Phys.*, 1985, vol. 59, p. 347.
25. Fanourgakis, G.S., Apra, E., and Xantheas, S.S., *Chem. Phys.*, 2004, vol. 121, no. 6, p. 2655.
26. Bresme, F., *J. Chem. Phys.*, 2001, vol. 115, p. 7564.
27. Neumann, M., *J. Chem. Phys.*, 1985, vol. 82, p. 5663.
28. Shevkunov, S.V., *Kolloidn. Zh.*, 2002, vol. 64, no. 2, p. 262.
29. Goggin, P.L. and Carr, C., Far Infrared Spectroscopy and Aqueous Solutions, in *Water and Aqueous Solutions*, Bristol–Boston: Adam Hilger, 1986, vol. 37, p. 149.
30. Nikitin, E.E., *Teoriya elementarnykh atomno-molekulyarnykh protsessov v gazakh* (The Theory of Elementary Atomic-Molecular Processes in Gases), Moscow: Khimiya, 1970.
31. Frenkel', Ya.I., *Kineticheskaya teoriya zhidkostei* (Kinetic Theory of Liquids), Leningrad: Nauka, 1975.
32. Tse, J.S. and Klein, M., *J. Chem. Phys.*, 1983, vol. 78, p. 2096.